5-1-2022

The effect of fin array height and spacing on heat transfer performance during pool boiling from extended surfaces

M. Winter

Justin A. Weibel
jaweibel@purdue.edu

2022 21st IEEE Intersociety Conference on Thermal and Thermomechanical Phenomena in Electronic Systems (iTherm) | 978-1-6654-8503-6/22/$31.00 ©2022 IEEE | DOI: 10.1109/iTherm54085.2022.9899575

The Effect of Fin Array Height and Spacing on Heat Transfer Performance during Pool Boiling from Extended Surfaces

Maureen Winter
Cooling Technologies Research Center
School of Mechanical Engineering, Purdue University
West Lafayette IN, USA
winter48@purdue.edu

Justin A. Weibel
Cooling Technologies Research Center
School of Mechanical Engineering, Purdue University
West Lafayette IN, USA
jaweibel@purdue.edu

***Abstract*—The use of heat sinks is a promising approach to extend the range of immersion cooling in dielectric fluids to higher heat fluxes for thermal management of next-generation electronics. However, the effects of extended surface area enhancement on the heat transfer performance under pool boiling conditions are not well understood, even in the simple case of straight fins. Further investigation of the heat-flux-dependent variation of boiling modes that can manifest along the fin height is required. Although approaches exist to predict the extended surface pool boiling heat transfer coefficient, they have been developed from single fins. As a result, when applied to fin arrays, they are rarely accurate across the full operating range up to the critical heat flux, particularly if height or spacing varies drastically. To better understand the effects of fin arrays on heat transfer, pool boiling experiments are performed using copper fins in water, varying fin height and spacing. These variations span a range from much larger to less than half of the scale of the capillary length scale, L_b. The pool boiling data, complemented with high-speed visualization of the boiling regimes and bubble dynamics, strongly support a hypothesis that L_b is the key length scale. Heat transfer from fin array heat sinks with heights and spacings above L_b are shown to be accurately predicted using existing fin analysis approaches from the literature. However, spacings smaller than L_b affect the nucleate boiling superheat while heights shorter than L_b are unable to support multiple boiling regimes along the fin sidewall, both leading to disagreement between the experiments and predictions. These aspects, coupled with observation of vapor entrapment between closely spaced fins, indicate that new predictive methods must be developed. The valuable insights offered into the effects of fin array height and spacing on pool boiling provide a pathway toward heat sink design optimization for immersion cooling applications.**

***Keywords*—pool boiling, heat sink, extended surface, fin array, critical heat flux**

I. Introduction

Two-phase immersion cooling provides an efficient means of heat dissipation to prevent overheating failures in electronics. The latent heat of the fluid absorbs large amounts of energy during the phase change, allowing the heat source to remain at a stable temperature. Generated vapor is then passively lifted away by buoyancy. However, the heat flux dissipated by immersion cooling is limited by critical heat flux (CHF), the point of transition from nucleate to film boiling where vapor completely covers and insulates the heated surface and causes a dramatic temperature increase. Therefore, because modern high-power electronics generate heat fluxes exceeding the CHF limit for all candidate working fluids, boiling surfaces must be enhanced.

Various boiling enhancement strategies have been extensively explored in the literature, as recently reviewed in [1–3]. One common enhancement approach involves microscale roughening [4–6] or coating the surface with porous structures [7, 8] to provide more nucleation sites, generally allowing for boiling heat transfer at a lower superheat. Use of nanoscale coatings has also garnered significant recent attention to achieve various enhancement effects, as reviewed in [9, 10]. The chemical wettability of a surface can further affect the boiling performance; highly wetting surfaces generally offer better CHF performance [11] whereas non-wetting surfaces favor increased nucleation density [12]. Recent efforts have developed surfaces with spatial patterns of different wettability [13, 14] or tailored the dynamic advancing and receding contact angles [15] to enhance boiling. However, despite these various surface enhancement strategies, low CHF values and long-term reliability of such coatings remain an issue.

Increasing the boiling surface area through use of extended surface heat sinks remains a simple and effective means to lower the heat flux. Yet, there is a comparatively small body of research that combines the benefits of extended surface area with surface enhancements [6, 16–18]. There is a need for understanding of boiling from macro-scale enhancement structures (i.e., extended fins) along with predictive methods for design of immersion cooling heat sinks.

Compared to a flat surface, pool boiling on extended surfaces allows for the boiling regime to vary along the fin height due to the temperature gradient. However, in heat sinks that typically comprise an array of closely spaced fins, physical confinement by the fins may affect the processes of bubble growth and departure. Both fin height and spacing are key length scales which affect these behaviors. First considering spacing effects, Park and Bergles [19] showed a trend of larger spacings achieving higher heat fluxes at lower superheats. Later, Yu and Lu [20] observed that closely packed fins promote nucleate

boiling at lower superheat, but can lead to a vapor layer developing at the base of the fins (dryout) at lower heat fluxes, confirming similar observations made for radial fins by Bondurant [21].

Regarding the effects of fin height, a common observation throughout the literature [6, 22–26] is that, as the heat flux increases, a vapor layer first develops over the surface at the base of the fin while nucleate boiling continues along the sides of the fin, thereby delaying the CHF compared to a flat surface. In general, heat sinks where only the fin height was varied showed consistent boiling performance until near CHF, where taller fins then outperformed shorter fins [6, 20]. Rainey and You [6] conducted an exhaustive study on roughened fins and noted that overly short of fins did not provide any extension of CHF, but the authors did not suggest a minimum height threshold; this study also observed that overly tall fins interfered with bubble departure, thereby increasing the superheat at a given heat flux, an observation later confirmed in [20].

Predictions of fin performance in pool boiling use the boiling curve from a flat surface to determine the heat transfer coefficient as a function of surface superheat, then assume this applies along the fin height regardless of any spacing or orientation effects. This approach was originally proposed by Haley and Westwater [25] and later used in [16, 22, 24, 27]; however, due to the limiting assumptions these predictions were not accurate for all fin dimensions and heat fluxes tested. Other predictions have used average heat transfer coefficients [6, 26]. Lai and Hsu [23] examined the varying regimes along the height, using the boiling incipience temperature to predict which portions of the fin would have nucleate boiling. These methods were also not accurate for all samples tested.

In summary, there is a need to determine why and when these pool boiling fin performance predictions can be accurately applied to heat sinks based on the array height and spacing. From previous spacing and height experiments [16, 21, 28, 29], we hypothesize that the bubble departure diameter, as characterized by the capillary length of the fluid, L_b, is the key length scale. Namely, both the array spacing, and the fin height, must be larger than this length for predictions to hold. Otherwise, bubble-fin interactions will cause significant deviations compared to the predictions. To this end, this study performs pool boiling experiments on a variety of fin arrays: spacing and height above, at, and below this length scale are tested. The measured boiling performance is then compared with fin analysis predictions to identify which cases have significant deviations. High-speed visualizations are used to relate the deviations to observations of the boiling regimes.

II. Experimental Methods

A. Facility Description

Experiments were conducted using water as the working fluid in the pool boiling chamber shown in Fig. 1. A detailed description of the chamber and the auxiliary flow loop are provided in [30] with the modified plenum of [31] used here.

To summarize, water is pumped with a gear pump at a low flow rate (~350 mL/min) from a reservoir into the chamber, shown in Fig. 1(a), made of polyether ether ketone (PEEK) walls with polycarbonate windows for visualization. At the inlet to the chamber, flow is evenly distributed into a polycarbonate plenum that has a solid plate mounted a short distance (3.17 mm) from

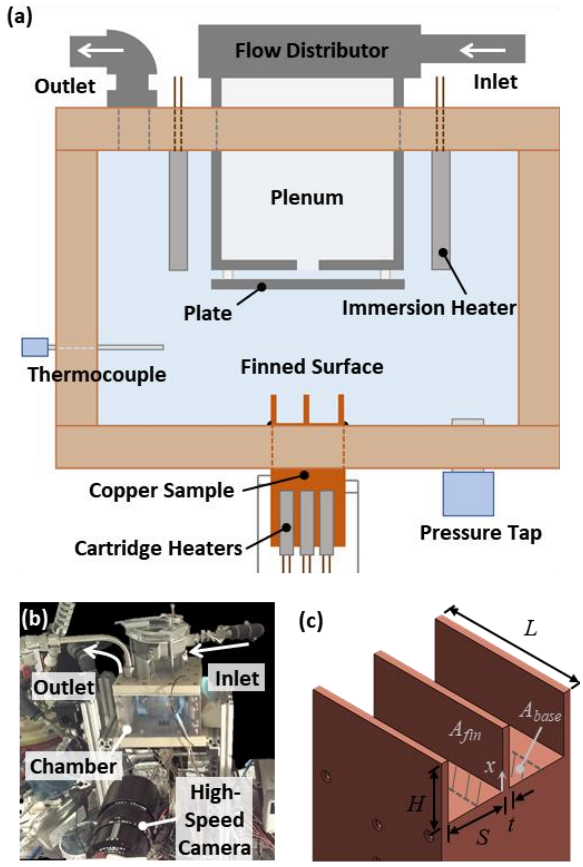

Fig. 1. (a) Schematic diagram of the chamber and (b) photograph of the pool boiling facility. (c) Heat sink sample with characteristic dimensions labelled.

the bottom, such that the radial outflow through the opening does not interfere with the boiling on the surface below. The chamber outlet returns to the reservoir, which contains Graham condensers open to the ambient that condense all vapor generated in the chamber. Saturated conditions are maintained in the chamber by supplementing the reservoir heaters with variable immersion heaters mounted from the top wall of the chamber. A T-type thermocouple and pressure transducer are used to ensure that the chamber stays at the saturation temperature at atmospheric pressure throughout the experiments.

The 20 mm × 20 mm footprint copper samples have longitudinal fins of rectangular profile, with characteristic height (H) and spacing (S) dimensions as shown in Fig. 1(c). The samples are inserted into the bottom wall of the chamber and sealed flush with a self-leveling adhesive (Q3-6611; Dow). To heat the samples, twelve 100 W cartridge heaters are embedded with even spacing into the bottom of the copper samples and connected to a variable power source. Three vertical thermocouple rakes are located along the front, middle, and back of the sample, with ice-point-referenced T-type thermocouples (uncertainty ±0.3 K) inserted. The rake along the centerline has four thermocouples spaced 2.54 mm apart; front and back rakes located 2 mm from the sides of the block have two thermocouples spaced 7.62 mm apart. The temperature gradients measured with these rakes are used to determine the

average input heat flux and extrapolated surface temperature (at the base of the fins) assuming one-dimensional heat flow in the sample.

B. Test Procedure

Before each experiment, the water was degassed by vigorous boiling in the reservoir and from the sample for at least 2 hr. The sample was then allowed to cool before starting the experiment. For each experiment, power to the sample was increased in steps of ~100-150 W, and the system allowed to reach steady state (a change in surface temperature of less than 1 K/hr). Steady state data at each power were recorded for 2 min at 0.5 Hz and then averaged. For some samples at high heat fluxes, typically in regimes with dryout at the base of the fins and nucleate boiling along the sides, it became evident that the steady state criterion was overly strict and was not reached after a long time (>2 hr). In these instances, data were instead recorded after waiting up to a maximum of 45 min for the temperatures to stabilize. Tests were stopped when CHF was reached, as indicated by a rapid temperature increase, or when the surface superheat exceeded 50 K. All data were supplemented with high-speed visualization (VEO710L; Phantom Vision Research).

C. Test Matrix

A test matrix was developed based on the bubble departure length scale, given by:

$$L_b = \sqrt{\frac{\sigma}{g(\rho_l - \rho_v)}} \quad (1)$$

where σ is the surface tension of the fluid, g is the acceleration due to gravity, and ρ_l and ρ_v are the liquid and vapor densities of the fluid, respectively. For water with all properties at the saturation conditions at atmospheric pressure, this length scale is ~2.5 mm. Seven samples were fabricated and tested with constant fin thicknesses (t) of 1 mm and different fin heights (H) and spacings (S) of either 1.0 mm, 2.5 mm, or 8.5 mm, as summarized in Table 1. These dimensions are intentionally lesser than, similar to, and larger than the bubble departure length scale, with the specific values chosen to yield 3, 5, or 10 evenly spaced fins along the 20 mm edge length of the boiling surface. Longitudinal fins were chosen to allow viewing of the bubble-fin interactions from the video.

Samples were additively manufactured from pure copper using a process (Markforged MetalX™) that results in a nominal post-sintering thermal conductivity of 350 W/mK per the manufacturer datasheet. A flat surface without fins was also fabricated and tested as a baseline using the same additive process. Each sample was cleaned prior to testing to remove any oils from handling during printing. Cleaning was performed in an ultrasonic cleaner using acetone and then isopropanol for 5 min each, followed by thorough rinsing in deionized water.

D. Fin Analysis Performance Prediction

The heat sink performance was predicted using a fin analysis with varying heat transfer coefficient along the fin as a function of the local wall superheat. This function, $h(\Delta T_w)$ as shown in Fig. 2, was determined using experimental results and established heat transfer correlations. For the nucleate boiling regime, the measured boiling data from the flat surface provided the heat transfer coefficient directly; this data was also used to determine the superheat range of the regime. The natural convection heat transfer coefficient was predicted assuming the upper surface of a horizontal plate using [32] while the film boiling regime heat transfer was predicted as in [22]. Film boiling superheat was taken from correlations developed by Berenson [33] for a large horizontal surface as described in [34]. The transitional boiling heat transfer coefficient was approximated to be a straight line between the maximum nucleate boiling heat transfer coefficient and the initial film boiling heat transfer coefficient, following the approach used for predictions in [22].

Following a standard fin analysis, the fin was discretized along its length into finite volumes and the set of control volume energy balance equations was iteratively solved to determine ΔT_w and h at each point. The boundary conditions

Table 1. Test matrix of heat sink samples. Each heat sink comprises an array of evenly spaced, longitudinal fins having a rectangular profile. The sample naming designates the fin height H and spacing S in millimeters.

Sample (Height-Spacing)	Parameter		
	Total Boiling Area to Footprint Ratio	H / L_b Ratio	S / L_b Ratio
H1.0-S8.5 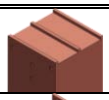	1.30	0.4	3.4
H2.5-S8.5 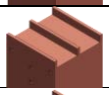	1.75	1.0	3.4
H8.5-S8.5 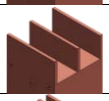	3.55	3.4	3.4
H8.5-S2.5 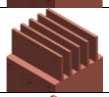	5.25	3.4	1.0
H8.5-S1.0 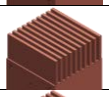	9.50	3.4	0.4
H1.0-S1.0 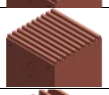	2.00	0.4	0.4
H2.5-S2.5 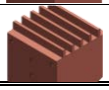	2.25	1.0	1.0

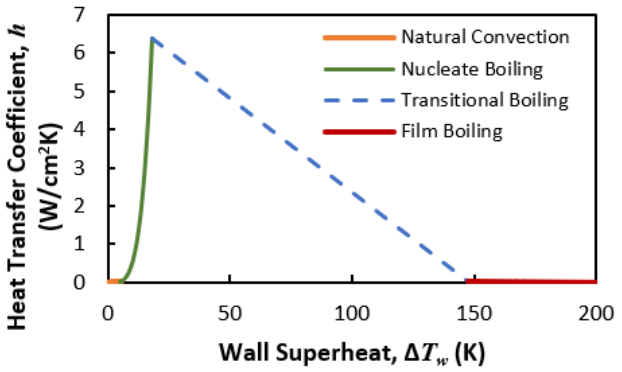

Fig. 2. Heat transfer coefficient as a function of wall superheat used as input to the fin prediction analysis.

were a fixed base temperature (as measured in the experiment) and convection from the tip of the fin. For the exposed base area between the fins, the base superheat was used to calculate the heat transfer coefficient. Once the final temperature distribution was determined, the total heat flux through each fin could be determined as

$$q'' = \frac{\sum_{x=0}^{x=H}(2h(\Delta T_w)\Delta T_w(x)(L+t)dx)+h(\Delta T_b)\Delta T_b SL}{A_{cell}} \quad (2)$$

where x is the position along the fin, L the width of the fin, dx the discretization size, ΔT_b the superheat at the fin base, and A_{cell} the footprint area of the repeating fin unit cell. This heat flux was then compared to experimental results for boiling from the finned surfaces.

III. Results

The effects of fin height (H) on the boiling curves are shown in Fig. 3, with the fin spacing held constant at a large S = 8.5 mm, over three times L_b. The experimental flat surface is also shown. The boiling curves plot the heat flux, q'', defined based on the 20 mm × 20 mm sample footprint as a function of base superheat, ΔT_b. In all the boiling curves presented herein, symbols are used to present the experimental data with lines of the same color showing the fin analysis predictions. Closed symbols are used for the data recorded after a fixed time interval, as discussed in the test procedure; a right-pointing arrow at the end of the curve indicates when the test was ceased due to a CHF excursion versus reaching a superheat limit. All fin heights have nearly identical performance, matching the flat surface as well as the predictions, up to the heat flux at which CHF is reached for the flat surface. The shortest 1.0 mm fins (H1.0-S8.5), having a height below L_b, reach CHF at nearly the same heat flux as the flat surface, despite the predictions suggesting that boiling could continue to higher fluxes. Above the CHF of the flat surface, the larger height fins of 2.5 mm and 8.5 mm have an inflection in the boiling curve then continue to boil up to higher heat fluxes, matching the behavior of the predictions. The predictions indicate that this inflection occurs when film boiling begins at the base of the fins, while the sidewalls continue in the nucleate boiling regime. Any distinction between the CHF for the 2.5 mm versus 8.5 mm tall fins cannot be resolved due to base superheats exceeding the temperature limit of 50 K before this transition occurs.

Fig. 4 shows the effects of spacing (S) on the boiling curves, with fin height held constant at a large H = 8.5 mm. Of the three runs, only the largest 8.5 mm spacing follows the predictions (sample H8.5-S8.5, as previously discussed in Fig. 3). The heat flux for the 2.5 mm spaced fins (H8.5-S2.5) is slightly overpredicted during the initial portion of the curve, and then significantly so past the inflection in the curve. The very close 1.0 mm spacing (H8.5-S1.0) is significantly underpredicted during nucleate boiling, and then slightly overpredicted past the predicted start of film boiling on the base surface. None of these samples reached CHF, and the experiments were stopped due to excess superheat, except for H8.5-S1.0, for which there was a cartridge heater failure that ended the test.

Another comparison in Fig. 5 shows the boiling curves for the samples with both height and spacing dimensions below, equal to, or above L_b. These three samples illustrate increasing discrepancies between the experimental data and predictions as the characteristic lengths are reduced. The H8.5-S8.5 sample generally has excellent agreement, in terms of the nucleate boiling superheat and point of inflection in the curve, while H2.5-S2.5 has slightly worse agreement both along the curve and with the point of inflection. The prediction appears unviable for H1.0-S1.0, which has poor agreement in the nucleate boiling regime and does not exhibit the predicted inflection.

To confirm that the boiling curve inflections correspond with the onset of film boiling at the base surface, particularly with

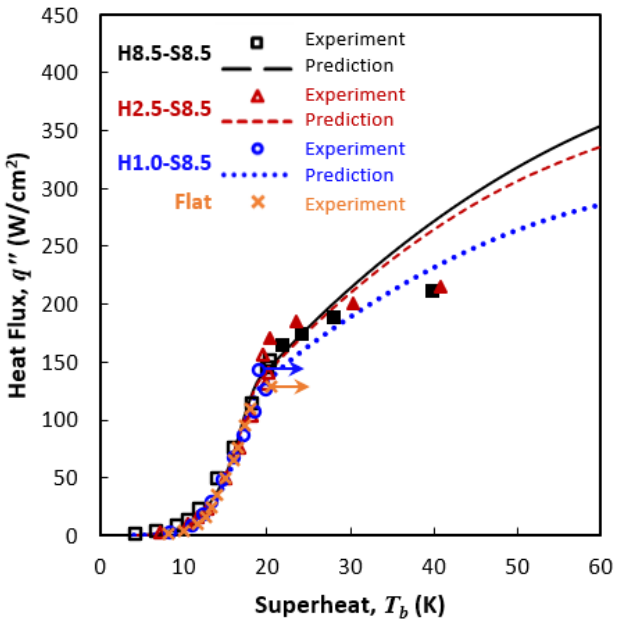

Fig. 3. Measured and predicted boiling curves for differing fin heights (H) at a constant S = 8.5 mm fin spacing.

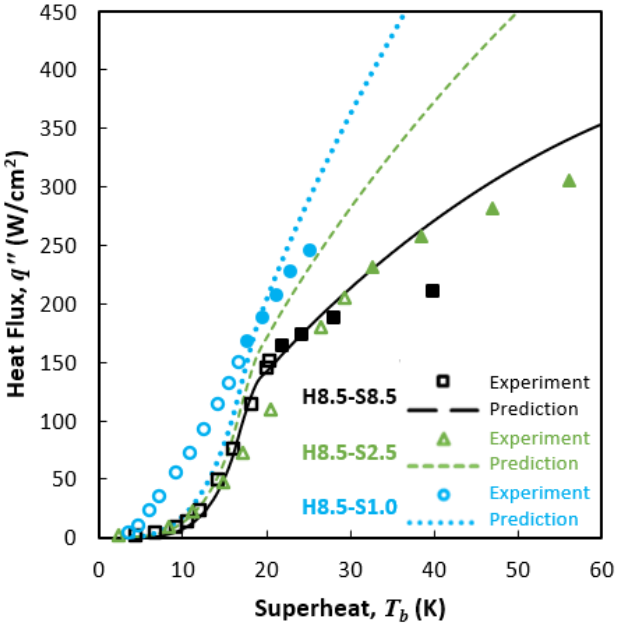

Fig. 4. Measured and predicted boiling curve for differing fin spacings (S) at a constant H = 8.5 mm fin height.

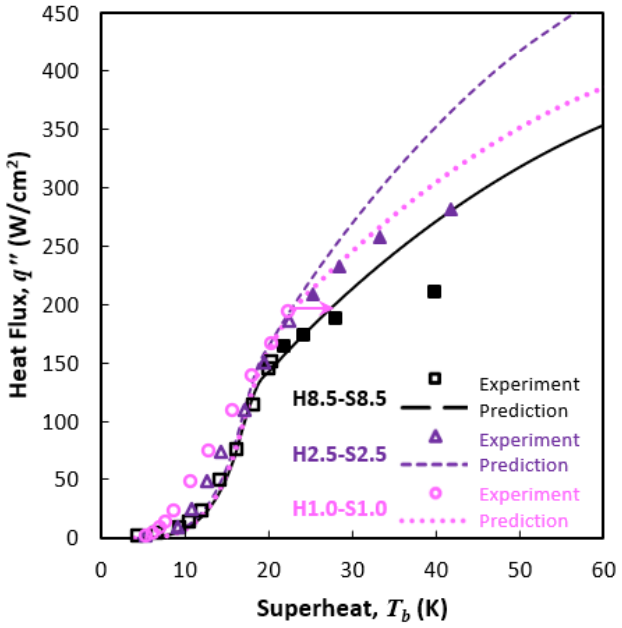

Fig. 5. Measured and predicted boiling curves for samples with equal height (H) and spacing (S) dimensions of 8.5 mm, 2.5 mm, and 1.0 mm.

varying the fin spacing, high-speed visualizations are examined in Fig 6 for different fin spacings at a fixed fin height of H = 8.5 mm. In each case, the top image is at a heat flux just below the predicted start of film boiling on the base surface, while the bottom image is the first heat flux above the inflection in the curve, corresponding with a filled symbol where the steady state criterion was not met within 45 min. Sketches below the image frames illustrate the location and morphology of the liquid-vapor interfaces near the base surface between the fins.

The sample with the largest spacing of S = 8.5 mm, shown in Fig. 6(a), has clear evidence of individual bubbles nucleating at the base of fins in at the lower heat flux of 114 W/cm^2. Moving to the higher heat flux, a stable vapor film completely covers the base surface between fins, and bubbles only nucleate from higher along the sidewall of the fin. The intermediate spacing of S = 2.5 mm, shown in Fig. 6(b), exhibits a similar behavior. However, due to the large amount of vapor billowing out of the front of the more tightly spaced fins, not every space between fins has clear indication of nucleate boiling from the base surface. Nevertheless, at the higher heat flux there is clearly a stable vapor layer completely covering the base with all nucleation events only occurring higher up the fin sidewalls. These two visualizations clearly confirm that the inflection in the boiling curve corresponds with coverage of the base with a vapor film.

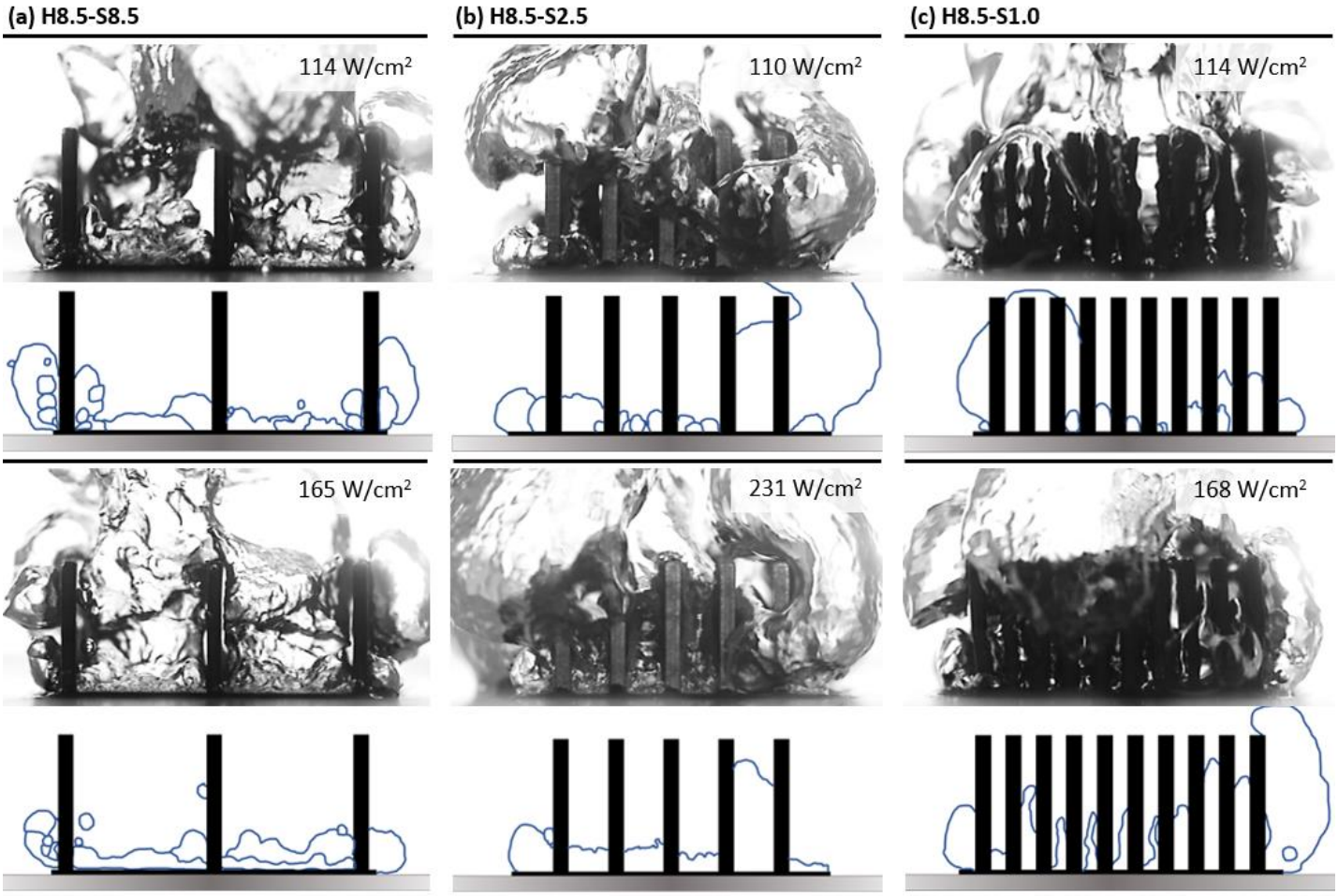

Fig. 6. High-speed flow visualization images and schematic illustration showing vapor morphology on the base surface for samples (a) H8.5-S8.5, (b) H8.5-S2.5, and (c) H8.5-S1.0.

For the most closely spaced tall fins, sample H8.5-S1.0, the predictions deviated most significantly from the experiments. While there was not a clear inflection in the experimental boiling curve data for this sample, the predicted slight inflection nevertheless corresponds with a key regime change as observed in the visualizations in Fig. 6(c). Albeit difficult to discern from a static image due to even more vapor billowing around the fins, the videos clearly show large bubbles nucleating from the corner between the fin and the base at 114 W/cm^2; these bubbles completely fill the space between the fins as they grow. At the higher heat flux of 168 W/cm^2, a constant film fills the spaces between the fins across the entire base.

For the two samples having the shortest fins with a height of H = 1 mm (H1.0-S8.5 and H1.0-S1.0), the boiling curve data showed that CHF was similar to the flat surface, with neither having an inflection in the boiling curve. The flow visualization image in Fig. 7 shows an example of such fins that are too short to have multiple regimes along the fin height, as the vapor film on the base surface completely envelops the fins.

IV. Discussion and Conclusions

For fin spacings larger than L_b, such as for the boiling curves shown in Fig. 3, it is clear that each fin acts independently and the fin height only affects the boiling curve at heat fluxes above the CHF of the flat surface. When examining the agreement between the experiments and fin analysis predictions, Fig. 3 also clearly shows that, for such far-spaced fins, it is accurate to assume that the heat transfer coefficient on the fin sidewalls can be approximated by the performance of the flat surface. This confirms that it is possible to describe boiling on the vertical sidewall of a fin as similar to a horizontal, flat surface, implying that orientation effects will be minimal for boiling heat sinks, as indicated by [27]. However, in order for the prediction to be reasonable past the inflection in the boiling curve where a vapor film forms over the base surface, the fins must be tall enough (at least the same as L_b) so that they are not enveloped by this film, as in the case of the shortest fins tested.

For a fixed fin height above L_b, small fin spacings below L_b strongly affect the boiling curve, leading to much lower superheats than would be predicted by a fin analysis in the nucleate boiling region, as is exemplified by the results in Fig. 4. It is theorized that this is related to the increased number of nucleation sites provided by the corners at the base of each fin and from confinement effects on the nucleating vapor bubbles, as shown by Fig. 6(c). Above the inflection in the boiling curve, where the base is covered by a vapor film and nucleate boiling occurs from the fin sidewalls, predictions were generally less accurate as spacing was reduced, indicating that for spacings smaller than L_b, the flat surface performance cannot describe the heat transfer coefficient from the fin sidewalls. New predictive approaches must be developed that account for fin interference during bubble departure for closely spaced fins. Although CHF was not reached for any of the tall fin samples tested in this work (those shown in Fig. 4), it is clear from the flow visualizations that closer spaced fins entrap more vapor within the heat sink. As vapor layers were shown to envelop the shortest fins and trigger CHF (as in Fig. 7), it is reasonable to speculate that closer spaced fins could reach CHF at lower heat fluxes, supporting the findings of [6, 20].

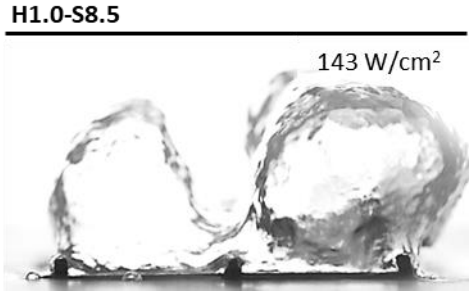

Fig. 7. Example visualization of the base vapor film enveloping short fins ($H < L_b$).

Overall, the results across this study support that the bubble departure length L_b is in fact a key length scale for the fin array. For fin heights and spacings larger than L_b, a fin analysis can be used to reasonably predict the heat sink performance using the boiling heat transfer coefficient as a function of superheat measured from a flat surface. At or below these length scales, the nucleate boiling heat transfer coefficient from the fin sidewalls does not follow this same function and a vapor layer develops over the base surface at significantly different heat fluxes. Further testing should be performed using additional working fluids with different L_b scales to show the generality of these conclusions.

Acknowledgment

Financial support for this work provided by members of the Cooling Technologies Research Center, a graduated National Science Foundation Industry/University Cooperative Research Center at Purdue University, is gratefully acknowledged. Maureen Winter acknowledges the National Science Foundation for support under the Graduate Research Fellowship Program (GRFP) under grant number DGE-1842166. The authors acknowledge Debraliz Isaac-Aragones help in running some of the experiments.

References

[1] U. Sajjad, A. Sadeghianjahromi, H. M. Ali, and C.-C. Wang, "Enhanced pool boiling of dielectric and highly wetting liquids – A review on surface engineering," *Appl. Therm. Eng.*, vol. 195, p. 117074, 2021.

[2] G. Liang and I. Mudawar, "Review of pool boiling enhancement by surface modification," *Int. J. Heat Mass Transf.*, vol. 128, pp. 892–933, 2019.

[3] W. Li, R. Dai, M. Zeng, and Q. Wang, "Review of two types of surface modification on pool boiling enhancement: Passive and active," *Renew. Sustain. Energy Rev.*, vol. 130, p. 109926, 2020.

[4] B. J. Jones, J. P. McHale, and S. V. Garimella, "The influence of surface roughness on nucleate pool boiling heat transfer," *J. Heat Transf.*, vol. 131, no. 12, p. 121009, 2009.

[5] M.-G. Kang, "Effect of surface roughness on pool boiling heat transfer," *Int. J. Heat Mass Transf.*, vol. 43, pp. 4073–4085, 2000.

[6] K. N. Rainey and S. M. You, "Pool boiling heat transfer from plain and microporous, square pin-finned surfaces in saturated FC-72," *J. Heat Transf.*, vol. 122, pp. 509–516, 2000.

[7] S. Sarangi, J. A. Weibel, and S. V. Garimella, "Quantitative evaluation of the dependence of pool boiling heat transfer enhancement on sintered particle coating characteristics," *J. Heat Transf.*, vol. 139, p. 021502, 2016.

[8] S. G. Liter and M. Kaviany, "Pool-boiling CHF enhancement by modulated porous-layer coating: theory and experiment," *Int. J. Heat Mass Transf.*, vol. 44, pp. 4287–4311, 2001.

[9] G. Liang and I. Mudawar, "Review of nanoscale boiling enhancement techniques and proposed systematic testing strategy to ensure cooling reliability and repeatability," *Appl. Therm. Eng.*, vol. 184, p. 115982, 2021.

[10] S. Bhavnani, V. Narayanan, W. Qu, M. Jensen, S. Kandlikar, J. Kim, and J. Thome, "Boiling Augmentation with micro/nanostructured surfaces: Current status and research outlook," *Nanoscale Microscale Thermophys. Eng.*, vol. 18, no. 3, pp. 197–222, 2014.

[11] C. M. Kruse, T. Anderson, C. Wilson, C. Zuhlke, D. Alexander, G. Gogos, and S. Ndao, "Enhanced pool-boiling heat transfer and critical heat flux on femtosecond laser processed stainless steel surfaces," *Int. J. Heat Mass Transf.*, vol. 82, pp. 109–116, 2015.

[12] T. P. Allred, J. A. Weibel, and S. V. Garimella, "Enabling highly effective boiling from superhydrophobic surfaces," *Phys. Rev. Lett.*, vol. 120, p. 174501, 2018.

[13] K. Ferjančič, M. Može, P. Križan, M. Bobič, and I. Golobič, "Subcooled critical heat flux on laser-textured stainless-steel ribbon heaters in pool boiling of FC-72," *Int. J. Heat Mass Transf.*, vol. 159, p. 120090, 2020.

[14] A. R. Motezakker, A. K. Sadaghiani, S. Çelik, T. Larsen, L. G. Villanueva, and A. Koşar, "Optimum ratio of hydrophobic to hydrophilic areas of biphilic surfaces in thermal fluid systems involving boiling," *Int. J. Heat Mass Transf.*, vol. 135, pp. 164–174, 2019.

[15] T. P. Allred, J. A. Weibel, and S. V. Garimella, "The petal effect of parahydrophobic surfaces offers low receding contact angles that promote effective boiling," *Int. J. Heat Mass Transf.*, vol. 135, pp. 403–412, 2019.

[16] I. Mudawar and T. M. Anderson, "Optimization of enhanced surfaces for high flux chip cooling by pool boiling," *J. Electron. Packag.*, vol. 115, pp. 89–100, 1993.

[17] I. Mudawar, "Assessment of high-heat-flux thermal management schemes," in *The 7th Intersociety Conference on Thermal and Thermomechanical Phenomena in Electronic Systems (ITherm)*, Las Vegas, NV, USA, 2000, pp. 1–20.

[18] I. Mudawar and T. M. Anderson, "Parametric investigation into the effects of pressure, subcooling, surface augmentation and choice of coolant on pool boiling in the design of cooling systems for high-power-density electronic chips," *J. Electron. Packag.*, vol. 112, pp. 375–382, 1990.

[19] K.-A. Park and A. E. Bergles, "Boiling Heat Transfer Characteristics of Simulated Microelectronic Chips with Detachable Heat Sinks," in *The 8th International Heat Transfer Conference (IHTC)*, pp. 2099-2104 1986.

[20] C. K. Yu and D. C. Lu, "Pool boiling heat transfer on horizontal rectangular fin array in saturated FC-72," *Int. J. Heat Mass Transf.*, vol. 50, pp. 3624–3637, 2007.

[21] D. L. Bondurant, "Performance of transvers fins for boiling heat transfer," *Univ. Ill. Urbana-Champaign*, p. 1-182, 1970.

[22] N. Abuaf, S. H. Black, and F. W. Staub, "Pool boiling performance of finned surfaces in R-113," *Int. J. Heat Fluid Flow*, vol. 6, no. 1, pp. 23–30, 1985.

[23] F.-S. Lai and Y.-Y. Hsu, "Temperature distribution in a fin partially cooled by nucleate boiling," *AIChE J.*, vol. 13, no. 4, pp. 817–821, 1967.

[24] D. R. Cash, G. J. Klein, and J. W. Westwater, "Approximate optimum fin design for boiling heat transfer," *J. Heat Transf.*, vol. 93, no. 1, pp. 19–23, 1971.

[25] K. W. Haley and J. W. Westwater, "Boiling heat transfer from single fins," in *The 3rd International Heat Transfer Conference (IHTC)*, 1966.

[26] F. Fantozzi, A. Franco, and E. M. Latrofa, "Analysis of the heat dissipation enhancement with finned surfaces in pool boiling of dielectric fluid," *Heat Mass Transf.*, vol. 36, pp. 487–495, 2000.

[27] G. Guglielmini, M. Misale, and C. Schenone, "Experiments on pool boiling of a dielectric fluid on extended surfaces," *Int. Commun. Heat Mass Transf.*, vol. 23, no. 4, pp. 451–462, 1996.

[28] T. M. Anderson and I. Mudawar, "Microelectronic cooling by enhanced pool boiling of a dielectric fluorocarbon liquid," *J. Heat Transf.*, vol. 111, pp. 752–759, 1989.

[29] G. J. Klein and J. W. Westwater, "Heat transfer from multiple spines to boiling liquids," *AIChE J.*, vol. 17, no. 5, pp. 1050–1056, 1971.

[30] M. J. Rau, T. Guo, P. P. Vlachos, and S. V. Garimella, "Stereo-PIV measurements of vapor-induced flow modifications in confined jet impingement boiling," *Int. J. Multiph. Flow*, vol. 84, pp. 19–33, 2016.

[31] C. Mira-Hernández, J. A. Weibel, and S. V. Garimella, "Visualizing near-wall two-phase flow morphology during confined and submerged jet impingement boiling to the point of critical heat flux," *Int. J. Heat Mass Transf.*, vol. 142, p. 118407, 2019.

[32] J. R. Lloyd and W. R. Moran, "Natural convection adjacent to horizontal surface of various planforms," *J. Heat Transf.*, vol. 96, no. 4, pp. 443–447, 1974.

[33] P. J. Berenson, "Film-boiling heat transfer from a horizontal surface," *J. Heat Transf.*, vol. 83, no. 3, pp. 351–356, 1961.

[34] C. Liu and T. G. Theofanous, "Film boiling on spheres in single- and two-phase flows.," Argonne National Lab., IL (US), DOE/ER/12933-3, 2000.